Canadian Science Publishing | Canadian Geotechnical Journal

Crack-resistant cement-bentonite cut-off wall materials incorporating superabsorbent polymers

Journal:	*Canadian Geotechnical Journal*
Manuscript ID	cgj-2020-0181.R2
Manuscript Type:	Article
Date Submitted by the Author:	29-Jul-2020
Complete List of Authors:	Cao, Benyi; University of Cambridge, Department of Engineering Chen, Jingtao; University of Cambridge, Department of Engineering Al-Tabbaa, Abir; University of Cambridge, Department of Engineering
Keyword:	cement-bentonite, crack resistance, superabsorbent polymer, wet-dry, microXCT
Is the invited manuscript for consideration in a Special Issue? :	Not applicable (regular submission)

Crack-resistant cement-bentonite cut-off wall materials incorporating superabsorbent polymers

Benyi Cao[1]*, Jingtao Chen[2], Abir Al-Tabbaa[3]

1* PhD candidate, corresponding author, Department of Engineering, University of Cambridge, Cambridge, CB2 1PZ, UK. E-mail: bc457@cam.ac.uk; Tel: +44(0)7410205759.

2 PhD candidate, Department of Engineering, University of Cambridge, Cambridge, CB2 1PZ, UK. E-mail: jc933@cam.ac.uk.

3 Professor, Department of Engineering, University of Cambridge, Cambridge, CB2 1PZ, UK. E-mail: aa22@cam.ac.uk.

Abstract: Preserving the integrity of cement-bentonite cut-off walls, particularly in aggressive environments, is critical to their serviceability in polluted sites. The hardened cement-bentonite material in cut-off walls is highly susceptible to desiccation and wet-dry cycles, commonly leading to cracking. The objective of the work presented in this paper was to develop crack-resistant cement-bentonite cut-off wall materials subject to wet-dry cycles. Superabsorbent polymers (SAPs), which are cross-linked polymers that can absorb and retain a large amount of water and swell as a result, were employed for this purpose. It is found that the added SAPs increased the compressive strength by decreasing the water to cement ratio, and that the strain at failure also increased due to energy dissipative and reinforcement effects. In addition, crack resistance was greatly improved under the imposed wet-dry cycles as the matrix suction was reduced as a result of the reduction of the contact between the free pore water and cement-bentonite particles and the increase of the pore size in the matrix. The morphology and microstructure of the interconnected foam network formed by the SAP films in the matrix were identified with SEM-EDX and micro-CT scan analyses. The results demonstrated the significant potential for SAPs in the development of crack-resistant cement-bentonite cut-off wall materials.

Keywords: cement-bentonite; crack resistance; superabsorbent polymer; wet-dry

Introduction

Cement-bentonite mixes have been widely used in cut-off walls initially for hydraulic cut-off in dam foundations and more recently for the containment of waste or contaminated ground (ICE, 1999). The mix composition differs from project to project although generally within a relatively narrow range. Bentonite slurry is usually prepared by mixing 3 to 6% bentonite with water and allowing the mix to hydrate for 24 hours. The binder, 100% Portland cement or blended with ground-granulated blast-furnace slag, is then added to the bentonite slurry at a dosage of 10 to 35% by weight to produce the cement-bentonite mix (Garvin & Hayles, 1999; Opdyke & Evans, 2005; Jefferis, 1981). Preserving the integrity of cement-bentonite cut-off walls, particularly in aggressive environments, is critical for their long-term durability and serviceability. The hardened cement-bentonite mixes employed are usually highly susceptible to desiccation and wet-dry cycles, leading to cracking and even disintegration (Tedd, 2005). When water is removed from the initially saturated cement-bentonite mix by evaporation, the air gradually enters the void space. Surface tension effects at the air-water-solid contacts inside the matrix generate negative pressures (matrix suction), leading to cracking when the induced tensile stress is equal to or greater than the tensile strength. Such cracking is irreversible and significantly increases the permeability of cut-off walls (Tedd, 2005). In the field, the effects of drying tend to be much more rapid and much more severe than are seen in the laboratory (Jefferis, 2012). It is reported the cement-bentonite samples collected in-situ from a cut-off wall in Yorkshire, UK, collapsed with an associated loss of structure upon drying (Philip, 2001). The portion of the cut-off wall near the groundwater table was particularly susceptible to wet-dry cycles due to seasonal fluctuations of the groundwater (Joshi et al., 2010). During the construction of a cut-off wall, evaluated by Cermak et al. (2012), vertical cracks were

observed in the borehole sidewalls at the locations of field permeability tests. It was observed that all cracks were essentially vertical and the widths ranged from approximately 0.5 mm to 1.5 mm. The crack surfaces were irregular and rough, and did not exhibit signs of shear distortion. It is therefore concluded that these cracks were attributed to drying cracking.

It is therefore important to develop resilient cement-bentonite materials that are crack-resistant to desiccation and wet-dry cycles over the lifetime of cut-off walls. The cracking could be mitigated or even eliminated by increasing the tensile strength of the cement-bentonite material and/or decreasing the tensile stress induced by desiccation or wet-dry cycles. Soil desiccation cracking is a common natural phenomenon, which has been studied extensively over decades (Peron et al., 2009; Li et al., 2011; Tang et al., 2018). Research methods that are applied in soil desiccation cracking tests to investigate the process and mechanism of desiccation cracking usually include the crack image capture device (Liu et al., 2013), CT scan (Tang et al., 2019), electrical resistivity method (Tang et al., 2018), and fibre-based sensing technique (Dong et al., 2019; Cheng et al., 2020). Recently, factors affecting the crack initiation and propagation (e.g., the specimen initial condition, size, thickness, mineral composition, environment temperature, specimen-container contact condition, fibre reinforcement and wet-dry cycles) are well studied and understood (Wang et al., 2018; Tang et al., 2012). For example, experimental observations in a CT scan test conducted by Tang et al., (2019) showed that cracks initiate at the surface, propagate both laterally and downward into the soil body, and transit into massive networks due to coalescence and bifurcation. This integrated approach is of great significance to characterise three-dimensional soil desiccation crack patterns and brings new perspectives into the study of the hydro-mechanical behaviour of clayey soils.

The reinforcement of soils using randomly distributed fibres for higher tensile strength has been performed for millennia (Hejazi et al., 2012). Stresses in the soil mobilise tensile resistance in the fibres, which in turn imparts greater strength to the soil. In previous studies, it was reported that the inclusion of polymeric fibres can reduce desiccation cracks in soils (Tang et al., 2012; Tang et al., 2016; Chaduvula et al., 2017). More recently, the application of microbial induced calcite precipitation (MICP) has been used for the mitigation of desiccation cracking in clay and bentonite soils (Vail et al., 2019; Liu et al., 2020). Liu et al. (2020) reported that under the MICP process, the densely distributed $CaCO_3$ crystal clusters on soil particle surface and inside inter-particle pores contributed to the improved mechanical integrity of soil sample as well as desiccation cracking resistance in cyclic wet-dry tests. The results obtained Vail et al., (2019) also showed the potential of MICP applications in the crack remediation for bentonite soils. These studies are expected to improve the fundamental understanding of desiccation cracking mechanisms in the MICP-treated soils and provide insights into the potential application of MICP for cracking remediation in clayey soils. However, despite the great potential and environmental benefits of MICP, its application to cement-bentonite mixes can be difficult for now because the highly alkaline environment and very low permeability of the cementitious matrix hinder the migration and biological activity of bacteria.

On the other hand, in cementitious materials all the water is rapidly drawn into the hydration process, and the surface tension within the capillaries causes autogenous shrinkage which can lead to cracking (Tazawa et al., 1995). This can be largely mitigated by introducing additional moisture for the enhancement of internal curing. Superabsorbent polymers (SAPs) are cross-linked polymers that can absorb and retain a large amount of water within a few minutes and swell to form a soft, insoluble gel

(Buchholz & Graham, 1998). When water molecules are drawn into the polymer network across a diffusion gradient, the polymer chains are not able to straighten, as they are cross-linked and as a result, water molecules begin to fill the empty spaces within the network, causing the particles to expand. The addition of SAPs in cementitious materials is a means of providing the extra curing water needed for cement hydration under low water-to-cement ratio conditions (Mechtcherine et al., 2014). The water released due to self-desiccation during cement hydration can be used for further hydration and reduction of the autogenous shrinkage (Snoeck et al., 2015; Kong et al., 2015). Jensen and Hansen (2002) measured up to 3700 microstrains (μm/m) of shrinkage in reference cement paste in a period of 3 weeks. When SAPs were used, there was successful mitigation of shrinkage and even some expansion. Snoeck et al., (2015) reported that SAPs with a mean diameter of 257μm were able to completely mitigate autogenous shrinkage in mixtures with a water-to-binder ratio of 0.30, with or without fly ash and/or blast-furnace slag as a supplementary cementitious material. Despite the extensive investigation on the improvement of crack resistance of cement and soil separately, research on the development of crack-resistant cement-bentonite mixes has not been presented in the literature before.

This study investigated the addition of SAPs in cement-bentonite cut-off wall materials for the improvement of crack resistance upon desiccation and wet-dry cycles. The effects of SAPs on the properties of cement-bentonite mixes were investigated in terms of their fresh properties (cement hydration and viscosity) and hardened properties (strength and permeability). A series of wet-dry cycle tests were carried out, and the cracking processes and the permeability after wet-dry cycles were examined to assess the improved crack resistance. The microstructure and morphology of SAPs embedded in cement-bentonite mixes were studied using a scanning electron microscope equipped

with an energy dispersive X-ray spectroscopy (SEM-EDX). In addition, X-ray micro-CT (micro-CT) scanning was used to investigate the distribution of SAPs and their interaction with the cementitious matrix, and the mechanisms of the improvement of crack resistance due to SAP addition were discussed.

Materials and methods

Materials and sample preparation

Cement-bentonite slurry was prepared using Portland cement (CEM-I 52.5 N, Hanson UK) and OCMA-grade bentonite (Macromin Kentish Minerals, UK). The chemical compositions of the cement and bentonite used are presented in Table 1. The control cement-bentonite slurry consists of 5% bentonite, 20% cement and 75% water (Jefferis, 1981), and the density of the slurry was ~1.2g/cm^3.

SAPs, supplied by BASF Chemicals, Germany, which is an acrylamide-acrylate copolymer, with particle size ~100 µm and a density of ~0.75 g/cm^3, was used in this study. The polymers have irregular particle shapes as they were produced via the bulk polymerisation technique, followed by crushing into single particles (Figure 1). The absorption capacity of the SAPs used was around 300g of deionised water/g of SAP and 20g filtered cement-bentonite slurry/g of SAP.

Water and bentonite were first mixed and left to hydrate for 24 hours. The cement and SAP particles were first dry mixed together for homogenous dispersion of SAPs. The cement, SAPs and hydrated bentonite slurry were then mixed together in a high-power mixer with a rotational speed of 190 rpm and motor power of 1200 watts for 10 minutes. The SAPs were added at three dosages of 0.2%, 0.6% and 1% by total weight of the cement-bentonite mixes. The cement-bentonite mixes containing SAPs were labelled by the proportion of SAPs added; e.g. SAP-0.2% refers to a cement-bentonite mix

containing 0.2% SAPs by total weight. The mixture was cast into cylindrical (50mm diameter and 100mm high) and disc (100mm diameter and 10mm high) moulds and cured in an incubator at a temperature of 20±2°C and relative humidity of 98±2% (Figure 2).

Testing methods

When the SAPs are added into the cement-bentonite mixes. there are a variety of observations and measurements that contribute to the overall performance of the system. This includes the effects of the added SAPs on the fresh and hardened properties of the material to ensure that the SAPs do not adversely affect the workability and properties of the cement-bentonite mixes, such as viscosity, strength, and permeability. The effects of SAPs on the fresh properties of the cement-bentonite slurry were investigated by examining the hydration process and viscosity of the mixes. The effects of SAP addition on the hardened mixes were investigated by conducting strength and permeability tests. In addition, the efficacy of crack-resistance performance was assessed through image analysis of the surface cracks and the maintenance of low permeability after several wet-dry cycles.

A Calmetrix I-Cal 2000 HPC High Precision Isothermal Calorimeter compliant with ASTM: C1679-14 (2014) was used to measure the heat of hydration for the cement-bentonite samples incorporating SAPs. Pre-conditioning of the cement, SAPs and bentonite slurry took place for 2 hours before all ingredients were mixed together for one minute. Logging of the heat of hydration and the cumulative heat production was carried out for 24 hours. A Brookfield DV3T Rheometer was used to measure the viscosity of cement-bentonite mixes. The viscosity testing method was adapted from Shahriar & Nehdi (2012). A shear stress versus shear rate relationship was obtained by subjecting the mix to shear rates varying from 46.5 to 232.5s^{-1} (ramp up) and back down

to 46.5s^{-1} (ramp down). The gradient of the shear stress versus shear rate relationship was then used to obtain the plastic viscosity.

The unconfined compressive strength (UCS) was determined based on ASTM: D4219-08 (2008) in triplicates using a Controls Testing Uniframe 70-T0108/E loading frame. The UCS and the strain at failure of the cement-bentonite mixes were tested at 28 days. UCS testing was started by applying a constant displacement rate of 1mm/min until failure. Also, a linear variable differential transformer was used to measure the vertical displacement of the specimen in order to obtain the strain at failure. The vertical permeability was determined by a constant flow rate test using flexible wall permeameters and peristaltic flow pumps according to ASTM: D5084-16 (2016), as shown in Figure 3. The cell water pressure was raised to 100kPa and maintained throughout the test. A steady flow rate was applied at the bottom of the sample using flow pumps. A pore pressure transducer positioned at the inflow position measured the pore water pressure generated, which was recorded by a data logger. When a constant pressure had been reached the vertical permeability of the sample was determined.

The wet-dry cyclic cracking test was performed after 28 days of curing. Samples were first dried in an oven at 40°C for 24 hours, and the first desiccation test was regarded as the completion of the first wet-dry cycle. The subsequent wetting was started by pouring distilled water directly into the mould. During this wetting process, sufficient water was provided to ensure full submergence for 24 hours at a room temperature of 20°C, after which the specimens were placed in the oven to be dried again. This procedure was repeated and finally a total of seven wet-dry cycles was applied to disc samples. After every cycle, the disc samples were taken out of the oven for image acquisition. For each image, the number and length of cracks on the disc samples were counted and measured using image processing software. First, the original colour

digital image was converted into 16-bit grayscale using ImageJ software. Then, by applying the binarisation operation using a simple gray threshold, cracks were separated from cement-bentonite matrix, after which the length and number of the cracks were measured in the binary image.

The scanning electron microscope (SEM) was used to characterise the microstructural surface morphology of the specimens and energy dispersive X-ray spectroscopy (EDX) was used to study the elemental composition. SEM images were taken of the control and SAP-containing cement-bentonite samples that were cured for 28 days. Small chipped pieces were collected from the specimens that were tested to failure during UCS tests. Phenom ProX SEM was used and the specimens were examined at a 10kV accelerating voltage. Micro-CT scan tests were conducted to investigate the microstructure and crack resistance mechanisms. The advantage of CT scanning is its ability to perform 3D imaging in a non-destructive way. It returns a 3D distribution of the local linear attenuation coefficient in the form of grey values, and specialized rendering software (VGStudio MAX) allows for visual inspection of this 3D volume. A specimen, 7mm×7mm×5mm, was cut from a SAP-1% disc sample and tested by X-ray micro-CT (Nikon XT H 225 ST) and its internal slice images were obtained through an image reconstruction process. A flat panel detector with 2000×2000 pixel was used and the four test parameters were set as follows: (i) X-ray energy: 70 kV and 85 mA, which are parameters determined by the sample geometry and the material composition; (ii) geometric magnification ratio: 39.5; (iii) reconstructed image matrix volume: 2000×2000×1000 voxels and (iv) effective voxel size: 5μm. The density of each voxel, represented by the material local linear attenuation coefficient, was normalized to 16-bit grey values. Image segmentation was then carried out to separate the digital image into multiple phases based on the difference in grey values of each phase.

Results

Effects on heat of hydration

The effect of the addition of the SAPs on the cement hydration processes in the bentonite slurry was investigated. The thermal powers produced per gram of cement for the first 24 hours are presented in Figure 4. The initial temperature of the test was set at 23°C and it was noted that during the testing period of 24 hours, the highest temperature recorded was 25°C. Such a slight increase in temperature had no effect on the physical and chemical properties of the SAPs and cement-bentonite materials. Generally, the addition of SAPs led to a slightly prolonged induction period and a delay in the thermal peak in the acceleration period. With 1.0% SAP content, the time to reach the thermal peak was delayed by 13% compared to that of the control mix. This indicates that the addition of the SAPs could alter the form and distribution of water in cement-bentonite mixes. The free pore water was homogeneously distributed in the matrix and thus readily available for hydrating cement particles. In contrast, the absorbed water was initially located inside the SAPs and hence could gradually migrate to the cement surface driven by osmotic pressure and humidity gradient. With the increased dosage of SAPs, more and more water was initially absorbed by the SAPs and therefore the water available in the early stage of the hydration process was reduced. With the consumption of free pore water due to cement hydration, the absorbed water was then gradually released by the SAPs. The release of water from the SAPs is a relatively slow process and therefore the reaction between the cement and water is slower than that of the control mix. Another reason for the retardation effect was that the surface of cement particles could have been covered by the swollen SAPs, preventing the exposure of the cement to free pore water.

Effects on rheological properties

Studies have reported that the addition of SAPs in cementitious materials increased the viscosity and reduced the workability as a result of the decreased water-to-cement ratio (Snoeck et al., 2015). The effects of SAP addition in cement-bentonite mixes were investigated and the variation in plastic viscosity and yield stress is presented in Figure 5. The plastic viscosity and yield stress showed an almost linear increase with the increasing SAPs content. The plastic viscosity of the cement-bentonite mixes containing 0.2%, 0.6% and 1.0% increased by 32%, 115% and 273%, respectively. As the flowability decreased, higher energy was needed to initiate the flow of the cement-bentonite slurry, thus increasing the yield stress. In the filtered cement-bentonite solution, the absorption capacity of the SAPs was ~20g/g, so the addition of 1% SAPs decreased the water-to-cement ratio from 3.75 (control) to 2.75. As the amount of free mixing water in the fresh cement-bentonite slurry decreases, reduction in workability is anticipated. For the cement-bentonite slurry used for cut-off wall construction, it is suggested that the plastic viscosity of the fresh slurry ranges from 12 to 78 mPa·s to achieve good workability (Ryan and Day, 1986). It should be noted that all the plastic viscosity values of SAP-containing mixes in this study were less than the suggested maximum value of 78 mPa·s. This means that the addition of the SAPs at a dosage of up to 1% is suitable, in terms of workability, for the construction of slurry trench cut-off walls.

Effects on mechanical properties

As shown in Figure 6, the addition of the SAPs increased the 28-day UCS of cement-bentonite mixes. An increase of 3%, 10% and 23% was observed for the SAP-0.2%, SAP-0.6% and SAP-1.0% mixes. This finding appears to contradict the common observation that the addition of SAPs in cementitious materials, in similar dosages to

those reported here, leads to a reduction in compressive strength, especially at early ages (Kong et al., 2014; Farzanian et al., 2016). The effect of SAP addition on the compressive strength is influenced by two counteracting mechanisms. On the one hand, the swollen SAPs can generate macro-pores in the cementitious matrix. These pores act as stress raisers to cause a localized lower strength and formation of cracks. On the other hand, the added SAPs absorb free mixing water and decrease the actual water-to-cement ratio. SAPs thus have both a positive and negative effect on the mechanical properties, which was also studied in Snoeck (2015). In previous studies, the reduction in UCS was observed in low water-to-cement ratio (0.3 to 0.5) mixes, in which the adverse effect of macro-pores generated by SAPs prevailed. However, the water-to-cement ratio used in this study is much higher at 3.75 for the control mix. Thus, a possible explanation for the increase in UCS of cement-bentonite is that when the water-to-cement ratio is relatively high, the addition of SAPs has a predominant beneficial effect on mechanical properties due to the reduced free mixing water. This also agrees with the work by Farzanian et al. (2016), reporting that the reduction in UCS of cement pastes by the addition of SAPs was more noticeable at lower water-to-cement ratios.

Another observed positive effect of SAP addition on the mechanical properties was the dramatic increase in the strain at failure. The addition of 0.2% SAPs appeared to have negligible effects on the strain at failure. In contrast, the strain at failure increased by 35% and 53% for SAP-0.6% and SAP-1.0% mixes, indicating that the SAP-containing samples were able to withstand a much larger deformation before they failed. The reason is twofold. First, the swollen SAPs can absorb a significant amount of strain energy and dissipate force by deforming and releasing water in compression. During the UCS tests of SAP-0.6% and SAP-1.0% mixes, beads of water were observed to

form on the surface of the samples, while this phenomenon was not encountered with the control samples. The beads were observed to form, grow and then flow down the surface as shown in Figure 7. These beads of water are a result of the compressed SAPs releasing the absorbed water, which can dissipate a considerable amount of applied force. The SAP particles formed a polymer network within the cement-bentonite matrix as revealed later in this paper. The absorbed water in the SAPs was released as the samples experienced the compressive stress during the UCS test. The water migrated within the polymer network of SAPs and moved fast to the outer surface of the samples. The absorption kinetics of the SAP particles, which governs the movement of water molecules in the SAP network, were tested in water, NaOH solution (0.1 mol/L), and a filtrated cement pore solution. In all the solutions tested, the absorption of the SAPs increased rapidly in the first 10 minutes and then stabilised after approximately only 20 minutes, indicating the fast movement of water in the SAPs. The second reason is the reinforcement provided by SAPs, which forms a polymer network within the matrix, as discussed in detail later.

Crack resistance

Digital images of the disc cement-bentonite samples were taken after each wet-dry cycle to assess the improvement of their crack resistance. In general, the cracks developed rapidly, with all the specimens except for the SAP-1.0% which exhibited at least one long straight crack in the first wet-dry cycle (Figure 8). It should be noted that, unlike soils, the cracks generated during drying in cement-bentonite mixes were not closed upon wetting. Such irreversible cracking makes the improvement in crack resistance very attractive for cement-bentonite cut-off walls because once the cracks initiate, they cannot be healed by wetting. The morphology of the crack patterns is significantly influenced by the addition of the SAPs. Figure 8 shows that the cracking

pattern of the control sample propagated in a three-pronged, T-like shape after the first cycle; however, the SAP-1.0% mix showed no evident cracks after the first cycle. After the 7th wet-dry cycle, the surfaces of control and SAP-0.2% were split into several separate irregular pieces by the formed crack segments, while only one to two cracks could be found on the SAP-0.6% and SAP-1.0% mixes. Most of the cracks stopped propagating when they were close to other existing cracks, and the predominant intersection nodes of cracks were of T-shape in the control samples and of Y-shape in the SAP-containing samples. The observation of T-shape intersections is consistent with the results reported by Tang et al., (2011a&b), where the intersection points of the cracks in clay soils are likely to form "T" and "+" shapes as the crack segments are generally perpendicular to each other and intersect at about 90°. This phenomenon can be interpreted on the basis of the crack propagation criterion described by Morris et al. (1992). Cracks tend to grow in the direction perpendicular to the local maximum tensile stress. Once the crack is initiated, the internal tensile stress perpendicular to the existing crack plane is released, and the direction of the maximum tensile stress becomes parallel to the plane of the existing cracks. As a result, the subsequent initial direction of the cracks that start at the existing cracks is perpendicular. In contrast, for the SAP-containing samples, the predominant intersection nodes of crack segments change from T-shape to Y-shape. This may be attributed to the bridging and reinforcement effect of SAPs, which changes the intrinsic development and release of the tensile stress field in the specimen, and as a result, changes the crack initiation and propagation. A similar transition of crack patterns was also observed in a fibre-reinforced clay soil (Tang et al, 2012).

The total crack lengths are shown in Figure 9 for quantitative analysis. Generally, the total length of crack decreased with the increase of the dosage of SAPs. A progressive

increase in total crack length from 132 to 260mm was observed in the control mix with the increase in the number of wet-dry cycles. This observation is consistent with crack patterns that are generally composed of the primary long main cracks and the subsequent short branch cracks. A similar final total crack length after seven cycles was obtained on SAP-0.2%, with the value rising sharply from 176 to 279mm in the fourth cycle. A marked improvement of crack resistance was noted in SAP-0.6% mix, where only one crack with a length of 87mm (around one-third of the final values of the control and SAP-0.2% mixes) appeared after the first cycle and no more cracking occurred over another six wet-dry cycles. The total crack length of SAP-1.0% mix remained the lowest before it increased abruptly to 170mm in the sixth cycle. Based on the final total crack length values after 7 wet-dry cycles, the dosage of 0.6% appeared to perform better than 1.0%, indicating the further increase in SAP dosage over 0.6% had no added benefit to crack resistance performance. This is probably because the excessively high SAP content could generate too many voids in the cement-bentonite mixes, leading to an increase in defects within the matrix and subsequent increased possibility of cracking.

The permeability was also measured on cylindrical samples subjected to only two wet-dry cycles, since after the second cycle the control samples deteriorated and could not be tested further. Figure 10 shows that the permeability of the control mix increased significantly, up to 6 times due to wet-dry deterioration after two cycles. The permeability of the SAP-containing samples increased by 4.0, 2.4 and 2.0 times its initial value for SAP-0.2%, SAP-0.6% and SAP-1.0% mixes respectively, suggesting the improved crack resistance in terms of permeability with the increase of SAP dosage. All the SAP samples remained intact, despite peeling, spalling and hairline cracks having appeared on the surface of the samples.

Cracking in cement-bentonite materials that are undergoing drying is controlled by matrix suction and by tensile strength. Surface-tension effects at the air-water-solid contacts generate negative pressures (i.e., matrix suction) below atmospheric pressure in the remaining pore water when the water content decreases (Morris et al., 1992). At a selected point, the cement-bentonite matrix tends to contract under the negative suction, and the matrix cracks when the induced suction is equal to or greater than the corresponding tensile strength. It is speculated that two positive effects of SAP addition have contributed to the improvement of crack resistance of the cement-bentonite mixes, i.e., the reinforcement effect and the suction reduction effect. First, the added SAPs swell and interlock cement-bentonite particles in the mixing process, forming an interpenetrating network of uncoiled SAP polymers, as shown in the SEM-EDX section later. This foam structure of SAPs act as reinforcement to increase the tensile strength of the cement-bentonite matrix. The bonding strength and friction between the SAPs and matrix enable the polymers to bear tensile stress that developed during drying, so the initiation of cracks can effectively be reduced. In addition to the increase of tensile strength provided by SAPs, the second factor contributing to the improved crack resistance is the suction reduction effect. Matrix suction, as defined in soil mechanics, is the attraction that the soil exerts on the water, and its magnitude is governed by the size of the voids: the larger the void, the smaller the curvature radius of the meniscus, and the lesser the attractive force (Fredlund, 2006). On the basis of the theory of unsaturated soil mechanics, the addition of SAPs might potentially reduce the matrix suction in two ways: (1) reduction of the contact between the free pore water and cement-bentonite particles and (2) increase of the pore size in the matrix. The contact between free pore water and cement-bentonite matrix is a prerequisite for the matrix suction. In SAP-containing mixes, the cement-bentonite particles are wrapped by SAPs,

which could absorb pore water and segregate the matrix from free water. The addition of SAPs could also create larger pores, which might increase the curvature radius of the meniscus and decrease the matrix suction as well. It should be noted that the matrix suction in the cement-bentonite mixed was not measured in this study, and the effects of SAP addition on the matrix suction should be verified by experiments in the future research.

SEM-EDX analysis

Representative SEM images showing the network structure of SAPs in the cement-bentonite matrix are presented in Figure 11. The SAP particles can be easily identified in the SEM images. They appeared dry and shrunk in films interconnected with one another, and part of these SAP films are firmly anchored in the matrix. The change in the structure and size of pores in cement-bentonite matrix due to SAP addition can be verified in the SEM images. SAPs were identified within voids in the cement-bentonite matrix, where the air space was believed to be created in the processes of the release of absorbed water and the shrinkage of SAPs. The SAP particles were saturated during the mixing of the cement-bentonite and the volume of the SAP particles expanded. During the drying process, the water retained in the SAPs was released as water vapour and the SAP particles gradually shrunk and created macro pores around them. The polymer backbone in SAPs is hydrophilic because it contained carboxylic acid groups, which attract polar water molecules when SAPs were added into cement-bentonite mixes. As shown in Figure 11, cement hydration products either precipitated on the surface of the SAP films, or were wrapped by the foam network of the SAPs. An EDX test was conducted on Point A on the surface of SAP films to analyse the chemical element composition. An evident trace of nitrogen confirmed that the SAPs were comprised of acrylamide and acrylate, and calcium and silicon detected on the SAP film indicated

good bonding between the cementitious particles and the hydrophilic polymers. This excellent adhesion laid the foundation for high bonding strength and friction between the SAPs and the cement-bentonite, providing reinforcement in the matrix and increasing the tensile strength. When the water content decreased in cement-bentonite, the matrix suction caused tensile stress and consequently mobilised tensile resistance in the polymer films, which in turn imparted greater strength to the cement-bentonite matrix. These randomly distributed SAP films acted as a three-dimensional network to interlock and link the cement-bentonite particles, and this deformable and soft network was able to slightly rearrange the cement-bentonite particles upon drying to eliminate stress concentration. A similar reinforcement effect was reported in fibre-reinforced soils (Tang et al., 2012).

As established earlier, another contributing factor to the improvement of crack resistance was the reduction in tensile stress (matrix suction) due to the addition of the SAPs. In comparison with the widespread small capillary pores in the control specimen as shown in Figure 12a, the pores in the SAP-1.0% specimens were generally larger macro-pores generated by the shrinkage of the SAPs upon drying (Figure 12b). The enlargement of the pore size effectively increased the curved water-vapour interfaces (menisci radii of curvature) and therefore could potentially decrease the capillary suction. In addition, the microstructure of the cement-bentonite matrix adjacent to SAP films was obviously improved as a result of the reduced amount of free pore water compared to the relatively loose cementitious matrix observed in the control specimen. In the SAP-1.0% specimen, the morphology of CSH gel was more condensed and a lower amount of portlandite and ettringite was produced, indicating a lower amount of free water present during hydration and curing processes. From these observations, it became apparent that the SAPs played an important role in the densification of the

hydration products and modification of their morphology by reducing the contact between cement-bentonite particles and free pore water. The insulation of cement-bentonite particles from free pore water impeded the formation of air-liquid-solid interfaces reducing the surface tension. The combination of enlargement of pore size and impediment of the formation of the air-liquid-solid interface significantly contributed to the reduction of the matrix suction and tensile stress in the SAP-containing cement-bentonite mixes.

Micro-CT scan analysis

High-resolution X-ray micro-computed tomography was conducted on a dried SAP-1.0% specimen to investigate the 3D morphology of the SAP network and the interaction between cement-bentonite and SAP films. The reconstructed CT images are the spatial distribution of the linear attenuation coefficients, which is expressed by grey scale values, with brighter regions (higher values of the grey level) corresponding to materials with a higher number of atoms and density. The dried SAP-1.0% specimen contained three phases: (1) an air phase of macro pores generated by the shrinkage of SAPs; (2) a light solid phase of shrunk SAP network; (3) a dense solid phase of cement-bentonite matrix. For the convenience of analysis, a region of interest, 3.3mm×2.3mm×2.2mm, was extracted and the representative 3D and 2D images are shown in Figure 13. Three phases can be obviously separated based on their different grey values: dense cement-bentonite particles appear in white and light grey, shrunk SAP films with a density of ~0.75 g/cm^3 appear in dark grey and air space with the lowest density appears in black.

Surface determination based on example areas was applied to calculate the threshold grey level values for different materials: a grey value of 7.5 separates the pores from the solid phase and a value of 54.5 further divides the solid phase into SAP films and

cement-bentonite particles. Based on these threshold values, pores, SAPs and cement-bentonite phases were coloured black, blue and brown respectively for the convenience of visual inspection (Figure 14). Large quantities of macro pores, which used to be filled with free pore water and swollen SAPs, can be clearly identified in the cross-section of the specimen. With the process of cement hydration, the absorbed water within the SAPs was gradually released to the surrounding matrix for further hydration reactions, and therefore these shrunken SAP particles created the macro pores in the matrix. These well distributed macro pores can contribute to the reduction of capillary suction in the drying process, decreasing the possibility of cracking of cement-bentonite. The brown cement-bentonite particles were normally found to be wrapped in blue SAP films, and the layer of SAPs act as a barrier between cement-bentonite and free pore water. As a result, the formation of the interface between free water and solid particles was obstructed and the surface tension was decreased. Transforming free pore water to absorbed water by SAPs plays a key role in reducing the matrix suction and improving crack resistance of cement-bentonite during drying. Reinforcement provided by SAP films can also be identified in the CT images. These films are interlocked and anchored in cement-bentonite matrix, and the bridging effect can effectively increase the tensile strength.

The foam structure of SAPs was extracted from the matrix to examine the distribution and morphology of the network (Figure 15). Dry SAP particles were added to cement-bentonite, and after mixing with water SAPs can form an interconnected network throughout the matrix, making the SAP-containing cement-bentonite mix a continuous medium rather than a dispersed one. This means the distribution of water content in the matrix is more homogeneous and the shrinkage due to the difference in water content could be potentially mitigated. Another benefit of the interconnection between SAP

films is that they can be firmly anchored in the matrix as a whole and therefore the reinforcement effect of SAPs was more uniform to further prevent the cracking caused by the uneven tensile reinforcement. Because of the interaction with hydrating cementitious particles, the voids in the foam network of SAPs are highly disordered in terms of both size and shape. However, the high flexibility of the disordered network of SAPs increases its spatial compatibility with the volumetric variation of cement hydration products. The SAP network has the ability to adjust water migration and uniformise water content in the whole matrix, which can reduce the differential drying and tensile stress.

Conclusions

This study developed crack-resistant cement-bentonite cut-off wall material incorporating a superabsorbent polymer (SAPs) subject to desiccation and wet-dry cycles. The main conclusions were:

1. The addition of SAPs in cement-bentonite had a slight retardation effect on the cement hydration process due to the fact that the release of absorbed water from SAPs is a relatively slow process.

2. The added SAPs absorbed mixing water and decreased the actual water-to-cement ratio of the cement-bentonite, thereby increasing its compressive strength. The strain at failure also increased due to the energy dissipative and reinforcement effects provided by SAPs.

3. Crack resistance was greatly improved by SAPs under wet-dry cycles. On the one hand, the reinforcement of SAPs increased the tensile strength; on the other hand, the matrix suction could be reduced as a result of the reduction of the contact between

the free pore water and cement-bentonite particles and the increase of the pore size in the matrix.

4. The morphology and microstructure of SAP films and their interaction with cement-bentonite matrix were revealed with SEM-EDX, confirming the reinforcement effect of SAPs. In addition, micro-CT scan analysis was used to reveal the interconnected foam network formed by SAP films in the matrix.

Data Availability Statement

Some or all data, models, or code that support the findings of this study are available from the corresponding author upon reasonable request.

Acknowledgement

The support from the EPSRC-funded programme grant Resilient Materials for Life (RM4L) (EP/P02081X/1) is gratefully appreciated. The first author would also like to acknowledge the support from the China Scholarship Council and Cambridge Trusts for his PhD study.

References

ASTM: C1679-14, (2014). Standard Practice for Measuring Hydration Kinetics of Hydraulic Cementitious Mixtures Using Isothermal Calorimetry. ASTM Int.

ASTM: D4219-08, (2008). Standard Test Method for Unconfined Compressive Strength Index of Chemical- Grouted Soils. ASTM Int.

ASTM: D5084-16, (2016). Standard Test Methods for Measurement of Hydraulic Conductivity of Saturated Porous Materials Using a Flexible Wall Permeameter. ASTM Int.

Buchholz, F. L., & Graham, A. T. (Eds.). (1998). *Modern superabsorbent polymer technology* (Vol. 152, p. 1). New York: Wiley-vch.

Cermak, Evans, & Tamaro. (2012). Evaluation of Soil-Cement-Bentonite Wall Performance—Effects of Backfill Shrinkage. Grouting and Deep Mixing 2012, 502–511.

Chaduvula, U., Viswanadham, B. V. S., & Kodikara, J. (2017). A study on desiccation cracking behavior of polyester fiber-reinforced expansive clay. *Applied Clay Science*, *142*, 163-172.

Cheng, Q., Tang, C. S., Zhu, C., Li, K., & Shi, B. (2020). Drying-induced soil shrinkage and desiccation cracking monitoring with distributed optical fiber sensing technique. Bulletin of Engineering Geology and the Environment, 1-12.

Dong, W., Li, W., Tao, Z., & Wang, K. (2019). Piezoresistive properties of cement-based sensors: review and perspective. Construction and Building Materials, 203, 146-163.

Farzanian, K., Teixeira, K. P., Rocha, I. P., Carneiro, L. D. S., & Ghahremaninezhad, A. (2016). The mechanical strength, degree of hydration, and electrical resistivity of cement pastes modified with superabsorbent polymers. *Construction and Building Materials*, *109*, 156-165.

Fredlund, D. G. (2006). Unsaturated soil mechanics in engineering practice. *Journal of geotechnical and geoenvironmental engineering*, *132*(3), 286-321.

Garvin, S. L., & Hayles, C. S. (1999). The chemical compatibility of cement–bentonite cut-off wall material. *Construction and Building Materials*, *13*(6), 329-341.

Hejazi, S. M., Sheikhzadeh, M., Abtahi, S. M., & Zadhoush, A. (2012). A simple review of soil reinforcement by using natural and synthetic fibers. Construction and building materials, 30, 100-116.

ICE (1999). Specification for the construction of slurry trench cut-off walls: As barriers to pollution migration. CIRIA Report Institution of Civil Engineers, Thomas Telford, London.

Jefferis, S. (2012). Cement-bentonite slurry systems. In *Grouting and Deep Mixing 2012* (pp. 1-24).

Jefferis, S. A. (1981). Bentonite-cement slurries for hydraulic cut-offs. In *Proceedings, Tenth International Conference on Soil Mechanics and Foundation Engineering, Stockholm, Sweden* (Vol. 1, pp. 435-440).

Jensen, O. M., & Hansen, P. F. (2002). Water-entrained cement-based materials: II. Experimental observations. Cement and Concrete Research, 32(6), 973-978.

Joshi, K., Kechavarzi, C., Sutherland, K., Ng, M. Y. A., Soga, K., & Tedd, P. (2010). Laboratory and in situ tests for long-term hydraulic conductivity of a cement-bentonite cut-off wall. Journal of geotechnical and geoenvironmental engineering, 136(4), 562-572.

Kong, X. M., Zhang, Z. L., & Lu, Z. C. (2015). Effect of pre-soaked superabsorbent polymer on shrinkage of high-strength concrete. *Materials and Structures*, *48*(9), 2741-2758.

Li, J. H., & Zhang, L. M. (2011). Study of desiccation crack initiation and development at ground surface. Engineering Geology, 123(4), 347-358.

Liu, B., Zhu, C., Tang, C. S., Xie, Y. H., Yin, L. Y., Cheng, Q., & Shi, B. (2020). Bio-remediation of desiccation cracking in clayey soils through microbially induced calcite precipitation (MICP). Engineering Geology, 264, 105389.

Liu, C., Tang, C. S., Shi, B., & Suo, W. B. (2013). Automatic quantification of crack patterns by image processing. Computers & Geosciences, 57, 77-80.

Mechtcherine, V., Gorges, M., Schroefl, C., Assmann, A., Brameshuber, W., Ribeiro, A. B., ... & Igarashi, S. I. (2014). Effect of internal curing by using superabsorbent polymers (SAP) on autogenous shrinkage and other properties of a high-performance fine-grained concrete: results of a RILEM round-robin test. Materials and Structures, 47(3), 541-562.

Morris, P. H., Graham, J., & Williams, D. J. (1992). Cracking in drying soils. *Canadian Geotechnical Journal*, *29*(2), 263-277.

Opdyke, S. M., & Evans, J. C. (2005). Slag-cement-bentonite slurry walls. *Journal of geotechnical and geoenvironmental Engineering*, *131*(6), 673-681.

Peron, H., Laloui, L., Hueckel, T., & Hu, L. B. (2009). Desiccation cracking of soils. European journal of environmental and civil engineering, 13(7-8), 869-888.

Philip, L. K. (2001). An investigation into contaminant transport processes through single-phase cement–bentonite slurry walls. *Engineering geology*, *60*(1-4), 209-221.

Pitt, M. J. (2000). The Marsh funnel and drilling fluid viscosity: a new equation for field use. SPE Drilling & Completion, 15(01), 3-6.

Pourjavadi, A., Fakoorpoor, S. M., Hosseini, P., & Khaloo, A. (2013). Interactions between superabsorbent polymers and cement-based composites incorporating colloidal silica nanoparticles. *Cement and Concrete Composites*, *37*, 196-204.

Ryan, C. R., and Day, S. (1986). Performance evaluation of cement-bentonite slurry wall mix design. Proc., National Conf. Hazardous Wastes, Hazardous Materials, Hazardous Materials Control Research Institute, Washington, DC.

Shahriar, A., & Nehdi, M. L. (2012). Optimization of rheological properties of oil well cement slurries using experimental design. Materials and structures, 45(9), 1403-1423.

Snoeck, D., Jensen, O.M., De Belie, N., (2015). The influence of superabsorbent polymers on the autogenous shrinkage properties of cement pastes with supplementary cementitious materials. Cem. Concr. Res. 74, 59–67

Tang, C. S., Shi, B., Cui, Y. J., Liu, C., & Gu, K. (2012). Desiccation cracking behavior of polypropylene fiber–reinforced clayey soil. *Canadian Geotechnical Journal*, *49*(9), 1088-1101.

Tang, C. S., Wang, D. Y., Cui, Y. J., Shi, B., & Li, J. (2016). Tensile strength of fiber-reinforced soil. *Journal of Materials in Civil Engineering*, *28*(7), 04016031.

Tang, C. S., Wang, D. Y., Zhu, C., Zhou, Q. Y., Xu, S. K., & Shi, B. (2018). Characterizing drying-induced clayey soil desiccation cracking process using electrical resistivity method. Applied Clay Science, 152, 101-112.

Tang, C. S., Zhu, C., Leng, T., Shi, B., Cheng, Q., & Zeng, H. (2019). Three-dimensional characterization of desiccation cracking behavior of compacted clayey soil using X-ray computed tomography. Engineering geology, 255, 1-10.

Tazawa, E. I., Miyazawa, S., & Kasai, T. (1995). Chemical shrinkage and autogenous shrinkage of hydrating cement paste. Cement and concrete research, 25(2), 288-292.

Tedd, P. (2005). Field Validation of Cement Bentonite Slurry Cut-Off Walls In Chemically Aggressive Ground At Gloucester Gasworks, *BRE Client report number 221-476*, Building Research Establishment Ltd.

Vail, M., Zhu, C., Tang, C. S., Anderson, L., Moroski, M., & Montalbo-Lomboy, M. T. (2019). Desiccation cracking behavior of MICP-treated bentonite. Geosciences, 9(9), 385.

Wang, L. L., Tang, C. S., Shi, B., Cui, Y. J., Zhang, G. Q., & Hilary, I. (2018). Nucleation and propagation mechanisms of soil desiccation cracks. Engineering Geology, 238, 27-35.

Figure Captions

Figure 1. Images of the SAPs used in this study (a) observed under an optical microscope and (b) an SEM image with EDX analysis of the chemical composition.

Figure 2. Cylindrical and disc cement-bentonite samples prepared as placed in an incubator.

Figure 3. The flexible wall permeameters used for permeability tests

Figure 4. The effect of SAP addition on the isothermal power of the cement-bentonite mixes.

Figure 5. The effect of SAP addition on the plastic viscosity and yield stress of the cement-bentonite mixes.

Figure 6. The effect of SAP addition on the UCS and strain at failure of the cement-bentonite mixes.

Figure 7. A SAP-containing cement-bentonite specimen being tested for UCS with highlighted beads of water.

Figure 8. Typical images of cracking patterns on disc cement-bentonite samples after the first and seventh wet-dry cycle.

Figure 9. Total crack length on the disc cement-bentonite samples after different wet-dry cycles.

Figure 10. The permeability of cement-bentonite samples after the first and second wet-dry cycle

Figure 11. Typical SEM-EDX results of (a) SEM image of interlocked cement-bentonite particles in SAP films and (b) EDX analysis of Point A on the SAP films.

Figure 12. Comparison between the microstructure and hydration products of (a) the control specimen and (b) the SAP-1% specimen

Figure 13. The reconstructed (a) 3D and (b) 2D image of the SAP-1% specimen.

Figure 14. Images of the SAP-1% specimen (the pores (black), the cement-bentonite matrix (brown) matrix and the SAPs (blue): (a) a 3D image; (b) a 2D image slice

Figure 15. CT scan 3D image reconstruction of the extracted SAP network

List of table

Table 1. Chemical compositions of the Portland cement and bentonite used, as provided by the supplier.

	Portland cement	**Bentonite**
SiO_2 (%)	19.5	54.2
Al_2O_3 (%)	4.9	18.8
CaO (%)	63.6	4.9
Fe_2O_3 (%)	3.1	5.0
MgO (%)	0.9	3.7
SO_3 (%)	3.3	--
Na_2O (%)	--	3.0
K_2O (%)	--	0.6

List of figures

Figure 12. Comparison between the microstructure and hydration products of (a) the control specimen and (b) the SAP-1% specimen

Figure 13. The reconstructed (a) 3D and (b) 2D image of the SAP-1% specimen.

Figure 14. Images of the SAP-1% specimen (the pores (black), the cement-bentonite matrix (brown) matrix and the SAPs (blue): (a) a 3D image; (b) a 2D image slice

Figure 15. CT scan 3D image reconstruction of the extracted SAP network

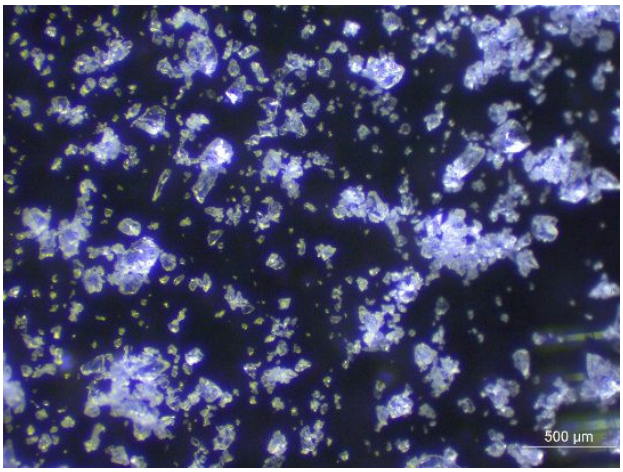

(a)

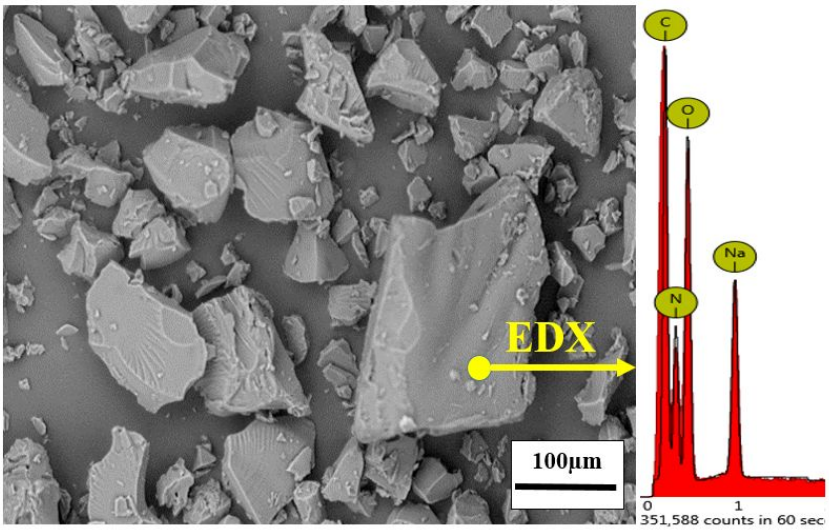

(b)

Figure 1. Images of the SAPs used in this study (a) observed under an optical microscope and (b) an SEM image with EDX analysis of the chemical composition.

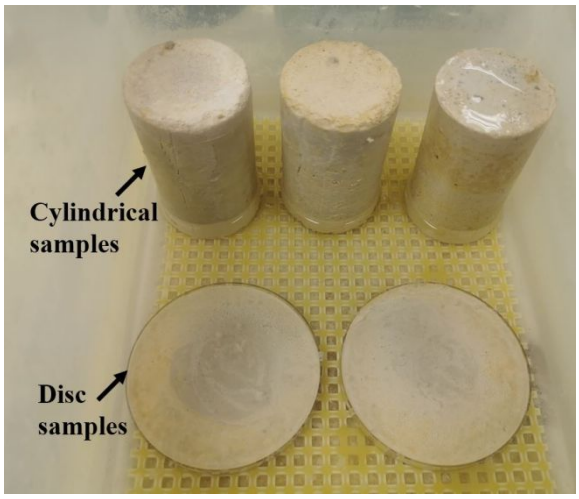

Figure 2. Cylindrical and disc cement-bentonite samples prepared as placed in an incubator.

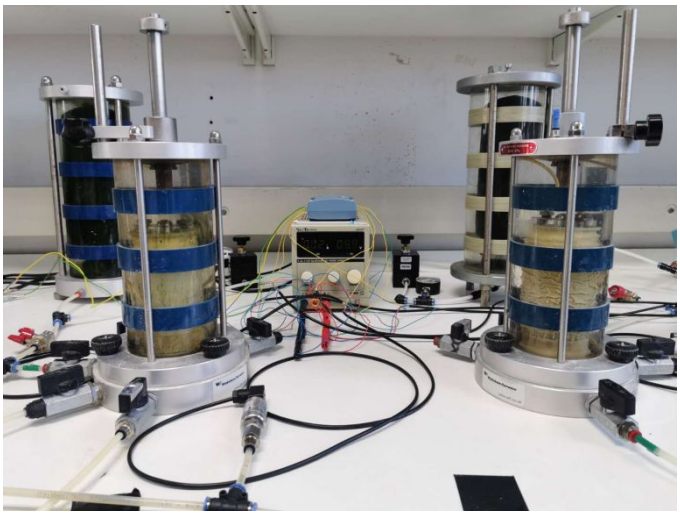

Figure 3. The flexible wall permeameters used for permeability tests

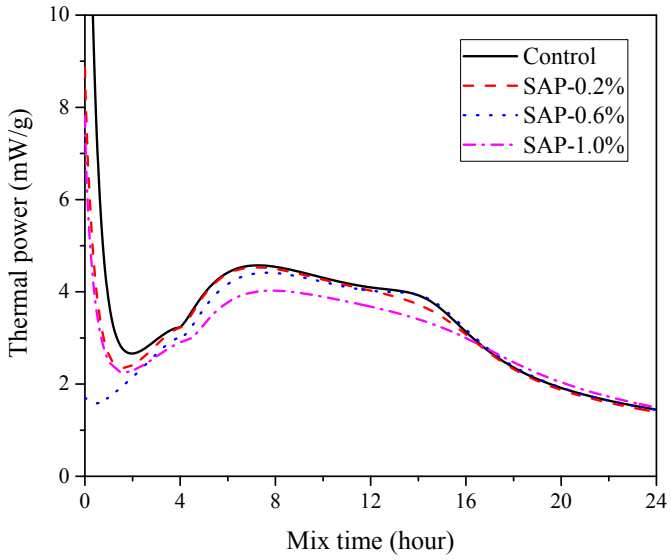

Figure 4. The effect of SAP addition on the isothermal power of the cement-bentonite mixes.

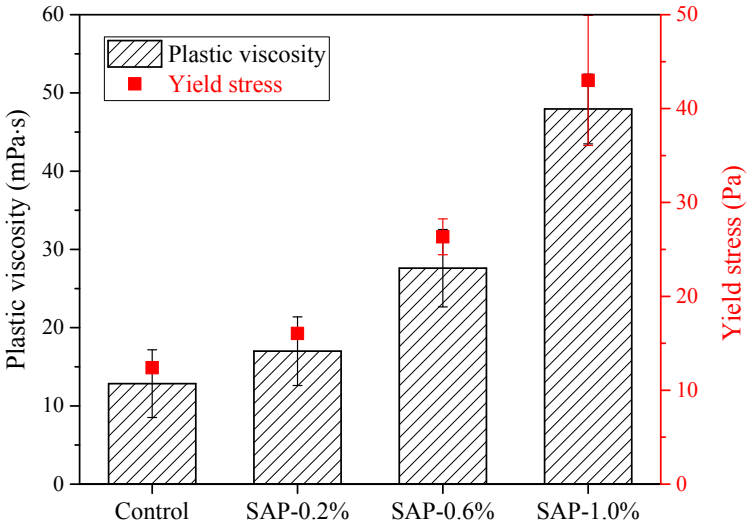

Figure 5. The effect of SAP addition on the plastic viscosity and yield stress of the cement-bentonite mixes.

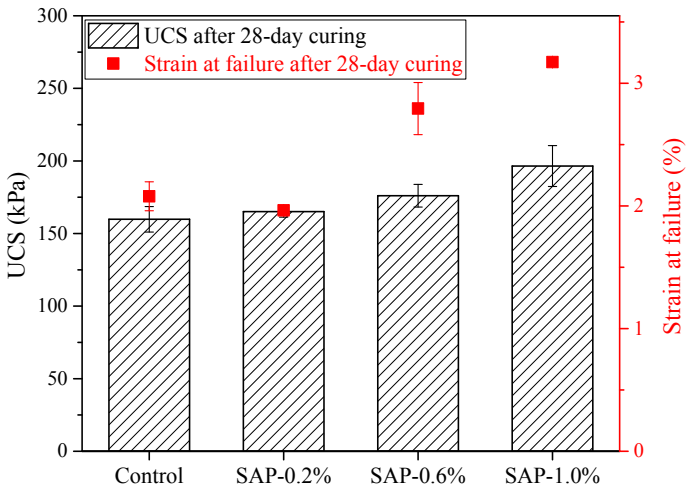

Figure 6. The effect of SAP addition on the UCS and strain at failure of the cement-bentonite mixes.

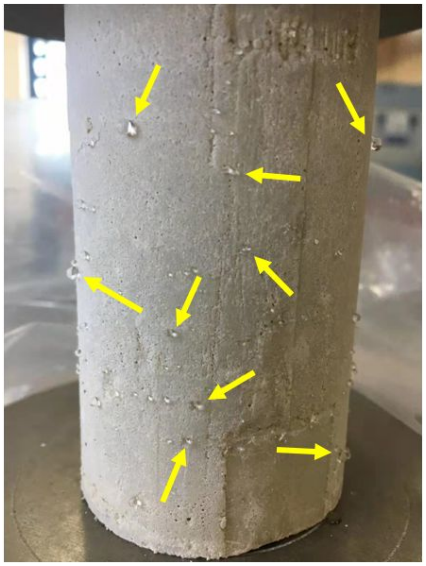

Figure 7. A SAP-containing cement-bentonite specimen being tested for UCS with highlighted beads of water.

Number of wet-dry cycles	Control	SAP-0.2%	SAP-0.6%	SAP-1.0%
1st wet-dry cycle		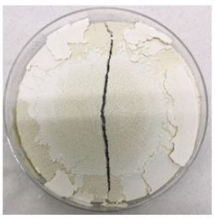	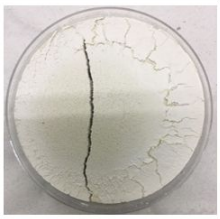	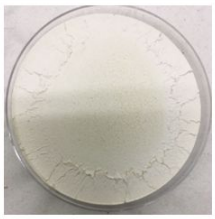
7th wet-dry cycle	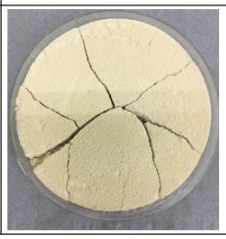			

Figure 8. Typical images of cracking patterns on disc cement-bentonite samples after the first and seventh wet-dry cycle.

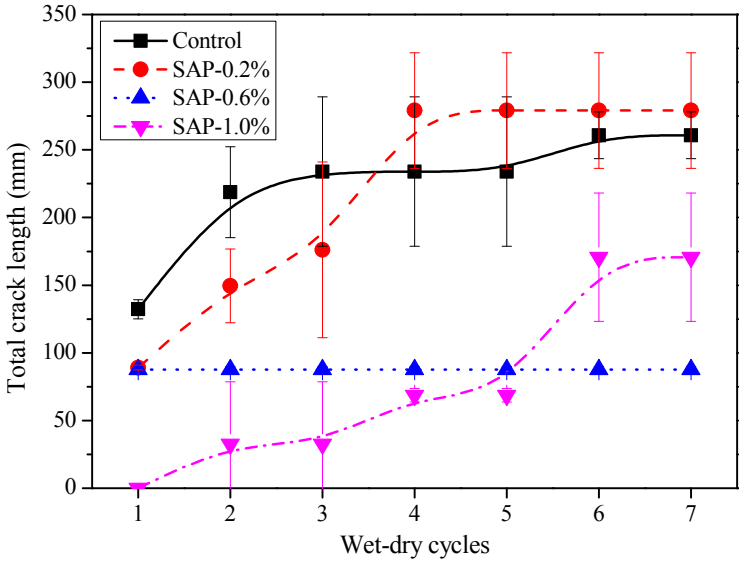

Figure 9. Total crack length on the disc cement-bentonite samples after different wet-dry cycles.

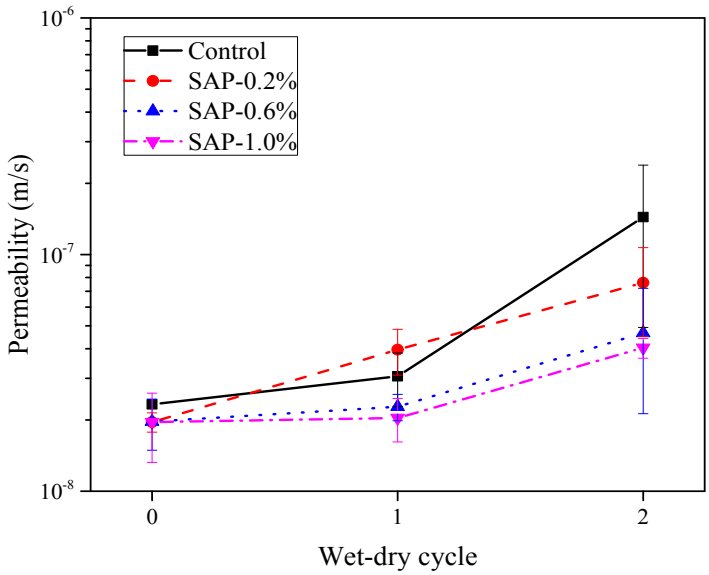

Figure 10. The permeability of cement-bentonite samples after the first and second wet-dry cycle

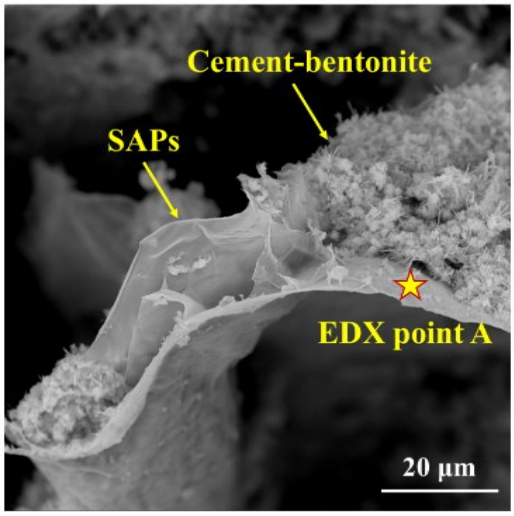

(a)

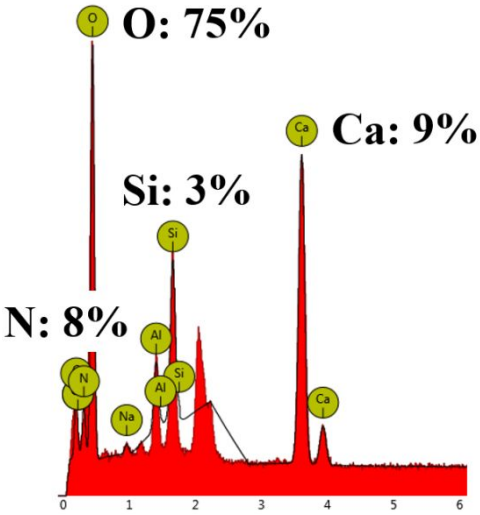

(b)

Figure 11. Typical SEM-EDX results of (a) SEM image of interlocked cement-bentonite particles in SAP films and (b) EDX analysis of Point A on the SAP films.

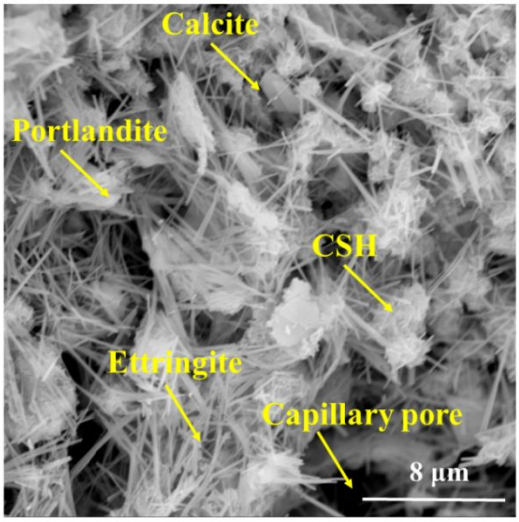

(a)

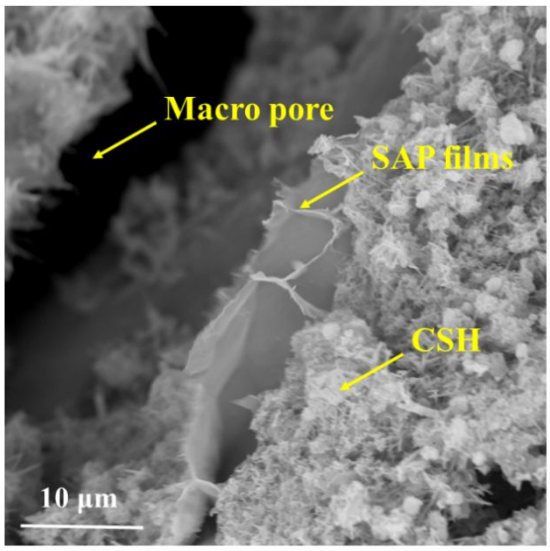

(b)

Figure 12. Comparison between the microstructure and hydration products of (a) the control specimen and (b) the SAP-1% specimen

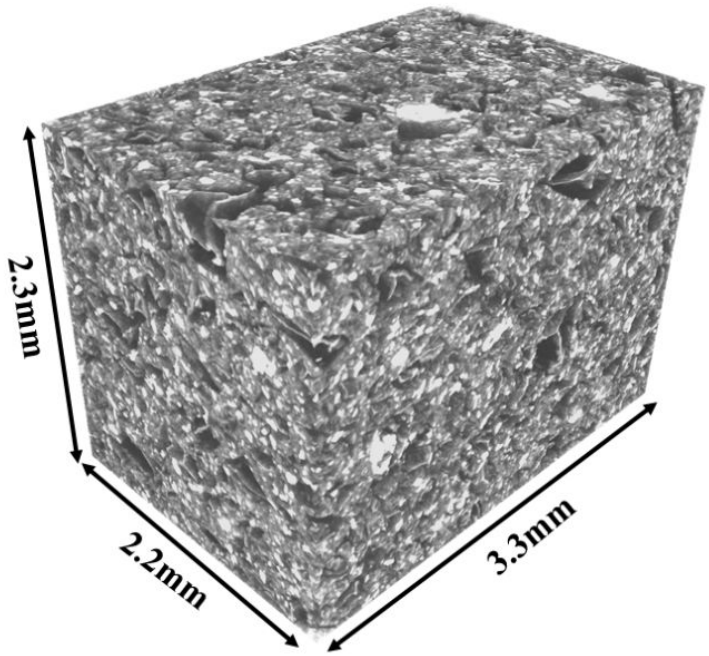

(a)

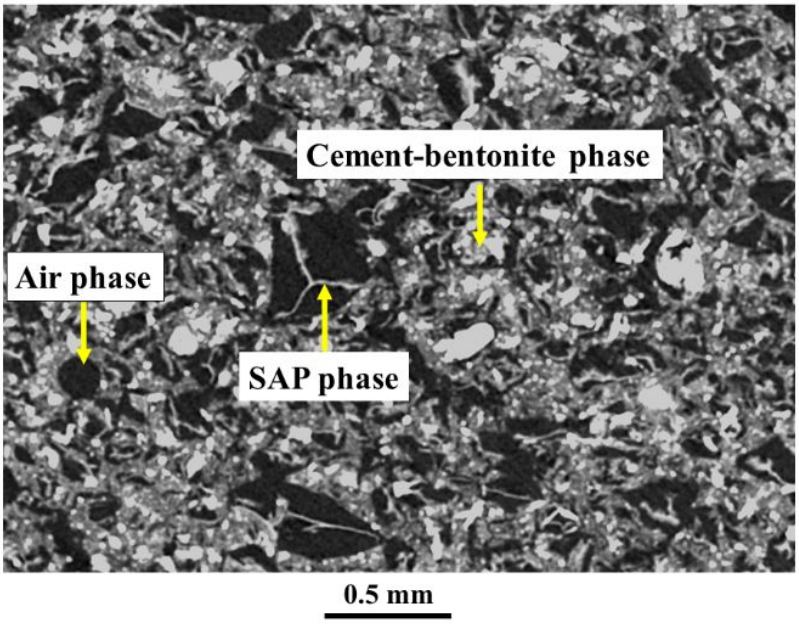

(b)

Figure 13. The reconstructed (a) 3D and (b) 2D image of the SAP-1% specimen.

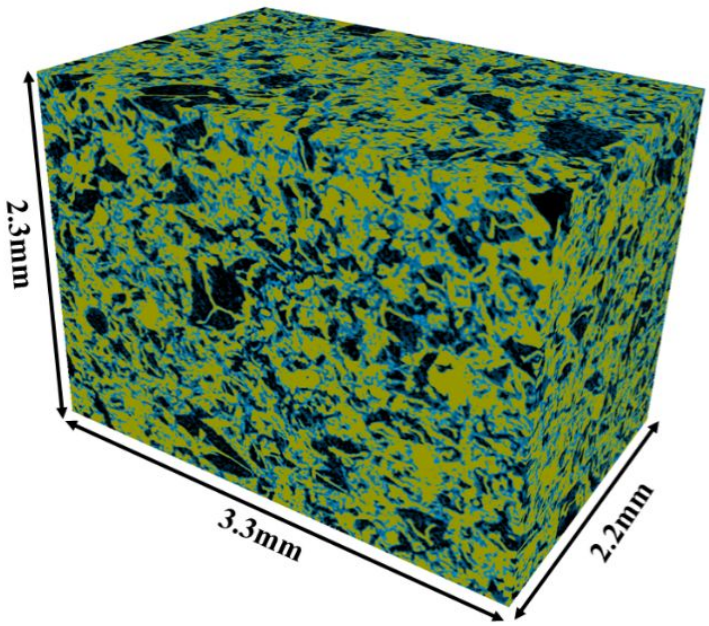

(a)

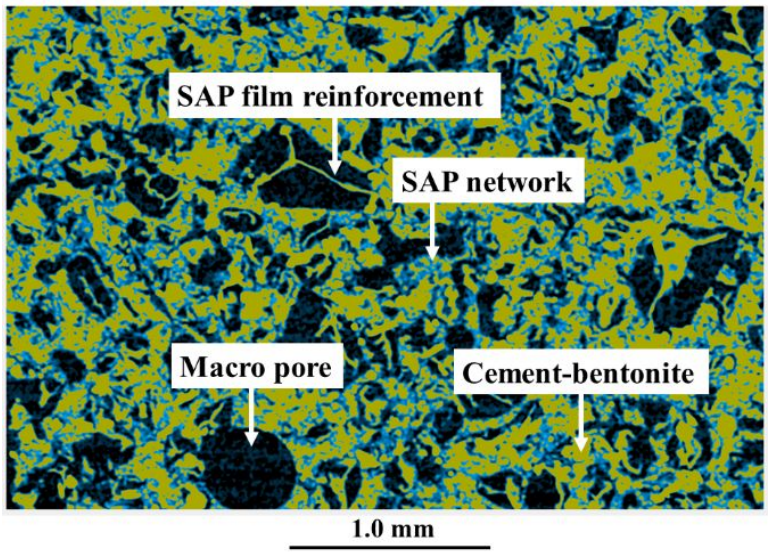

(b)

Figure 14. Images of the SAP-1% specimen (the pores (black), the cement-bentonite matrix (brown) matrix and the SAPs (blue): (a) a 3D image; (b) a 2D image slice

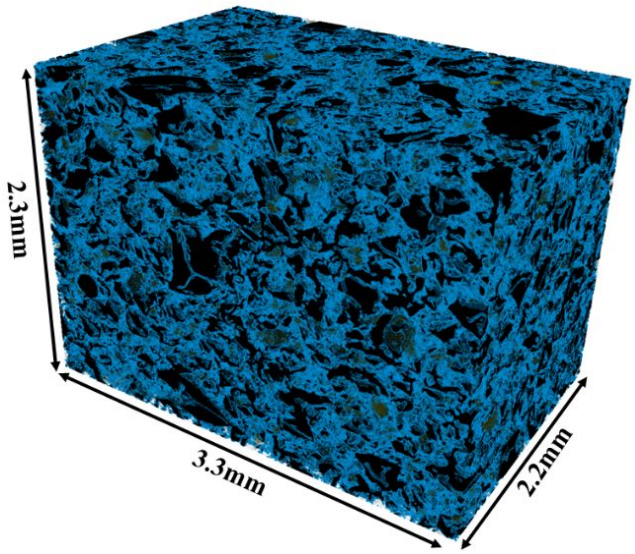

Figure 15. CT scan 3D image reconstruction of the extracted SAP network